# vuv frequency-comb spectroscopy of atomic xenon

Akira Ozawa* and Yohei Kobayashi†

*The Institute for Solid State Physics, The University of Tokyo, 5-1-5 Kashiwanoha, Kashiwa, Chiba 277-8581, Japan and CREST, Japan Science and Technology Agency, K's Gobancho, 7, Gobancho, Chiyoda-ku, Tokyo 102-0076, Japan*

(Received 11 December 2012; published 19 February 2013)

Direct frequency-comb spectroscopy of a single-photon transition ($5p^6$-$5p^5 6s$) in $^{132}$Xe is performed with a vacuum ultraviolet (vuv) frequency comb at 147 nm. The vuv comb is generated from an Yb-doped fiber laser system at a repetition rate of ∼79 MHz via high harmonic generation in a Kr gas jet placed at the focus point of an external enhancement cavity. For Doppler-reduced spectroscopy, a collimated atomic beam of isotope-selected $^{132}$Xe is used as a target. Repeated measurements with different repetition frequencies and highly sensitive time-resolved detection allow us to determine the absolute transition frequency with an uncertainty of 140 MHz in the vuv region.

DOI: 10.1103/PhysRevA.87.022507 PACS number(s): 32.30.Jc, 42.62.Eh

Spectroscopic studies have triggered the evolution of many new fields in physics. More than a century ago, investigations on atomic spectra prompted the formation of the old quantum theory and to this day high-precision laser spectroscopy makes important contributions in atomic and molecular science. In the past decade, the advent of the optical frequency comb has enabled significant progress in high-precision spectroscopy and frequency metrology; the $1S$-$2S$ transition frequency in atomic hydrogen has now attained a fractional frequency uncertainty of $4.2 \times 10^{-15}$ [1]. The determination of the Sr clock transition frequency relative to a Cs standard poses strong limits on the gravitational-coupling coefficients of various fundamental constants [2]. Moreover, broadband spectroscopy with frequency combs in the molecular-fingerprint region is expected to have many practical applications in medical and environmental diagnosis techniques [3,4]. However, the spectral coverage of conventional frequency combs based on mode-locked lasers is often limited to the visible to near-infrared region. Significant efforts have been made to introduce advanced comb metrology into previously unexplored wavelength regions such as the mid- and far-infrared or the vacuum ultraviolet (vuv) [5–9]. The latter is particularly interesting because high-precision vuv spectroscopy of light ions ($He^+$,$Li^{2+}$) promises stringent tests of higher-order corrections to bound-state QED [10] and because laser cooling and trapping of several atomic species in the vuv may enable investigations of basic reactions of organic chemistry with cooled carbon and hydrogen in a controlled way [11]. Although the first demonstration of a vuv frequency comb with the help of an external enhancement cavity dates back to 2005 [6,7], it is only very recently that a generated full rep-rate vuv comb has been applied to spectroscopy; Cingöz *et al.* demonstrated the comb-resolved spectroscopy of Ar and Ne at below 100 nm by utilizing a high-power vuv frequency comb [12].

In this study, we present direct frequency-comb spectroscopy of the single-photon transition of atomic xenon from the ground state to the first excited state ($5p^6$-$5p^5 6s$) at 147 nm [Fig. 1(a)]. Xenon has nine stable isotopes in natural abundance; a systematic investigation of those isotope shifts would allow us to test the Hartree-Fock calculations of the coupling between the nucleus and the surrounding electrons. Furthermore, the series of stable isotopes of Xe contains a magic nucleus ($^{136}$Xe) so that possible anomalies in the isotope shift associated with the closed neutron shell could be also investigated [13]. Because the transition is strongly allowed, a xenon discharge lamp has a prominent emission at 147 nm that can be used as an incoherent light source in the vuv region and has found commercial application in plasma display panels. Precise knowledge of the transition frequency makes it possible to use the emission as a convenient frequency reference; for example, to calibrate a vuv spectrometer. The last direct measurement of the transition was reported half a century ago by means of a high-resolution grating spectrometer and a xenon-discharge lamp [14]. Here, we show that by utilizing a vuv frequency comb, the transition frequency can be determined with significantly improved accuracy. Spectroscopy of atomic Xe with a vuv frequency comb entails the following difficulties: First, the vuv frequency comb is produced via high harmonic generation (HHG) by taking the 7th harmonic of an Yb-doped fiber laser based infrared frequency comb at 1030 nm. Although the wavelength is at the peak of the gain spectrum, it is close to the absorption edge of the medium as well. Therefore it is challenging to operate the power amplifier without introducing spectral narrowing and amplified spontaneous emission (ASE). Second, the xenon atomic beam has to be maintained at a low atom density to prevent the formation of clusters. Third, for spectroscopy of Xe, an atomic species other than Xe has to be employed as the target medium for HHG to prevent reabsorption of the generated vuv comb on the way to the spectroscopy chamber. When we used krypton instead of xenon for HHG, we found that the typical average power of the vuv comb was reduced by more than an order of magnitude which we attribute to the lower polarizability and the larger ionization potential of krypton. For these reasons, the expected spectroscopy signal is weak and a sensitive detection setup with low background noise is required. We show that our setup for vuv frequency-comb generation and spectroscopy has sufficient sensitivity and long-term stability to perform comb-resolved spectroscopy at a power level of as low as ∼500 fW per comb mode.

*ozawa@issp.u-tokyo.ac.jp
†yohei@issp.u-tokyo.ac.jp

 

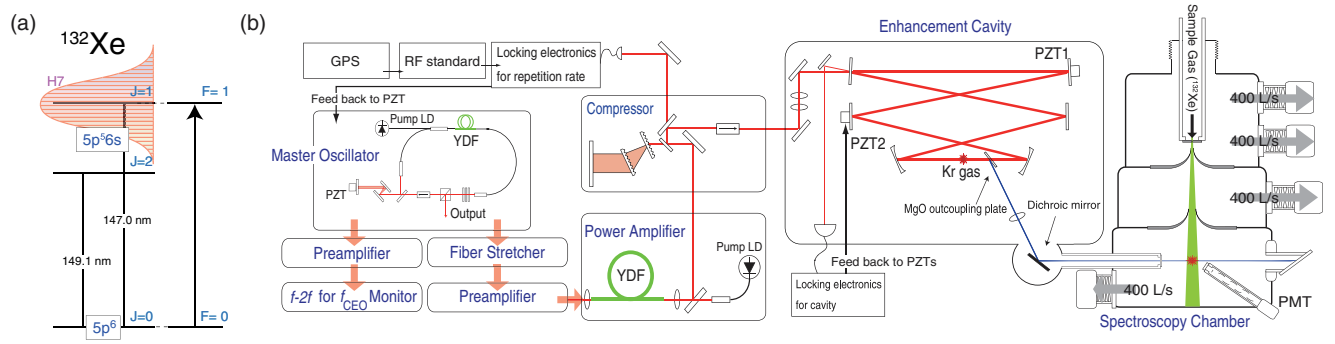


FIG. 1. (Color online) (a) Energy level diagram of $^{132}$Xe. The broadband excitation laser centered at 147 nm overlaps spectrally with a single excited state ($5p^5 6s$) without hyperfine splitting. (b) Schematic of the setup for vuv comb generation and comb-resolved spectroscopy.

Figure 1(b) shows the experimental apparatus. The vuv frequency comb is generated by cavity-enhanced HHG driven by an Yb-fiber laser system. The setup consists of a master-oscillator power-amplifier system, an enhancement cavity for HHG, and a spectroscopy chamber. The master oscillator is an Yb-doped fiber oscillator mode-locked by nonlinear polarization rotation. The output from the oscillator (pulse duration: 30 fs; average power: 10 mW) is sent into a fiber stretcher that prolongs the pulse duration to about several ps to prevent nonlinear effects in subsequent amplification stages. To efficiently amplify the weak oscillator output without introducing ASE, a low doping level gain fiber is employed in a preamplifier to boost the oscillator output up to 50 mW, which is sufficient to seed the power amplifier. In the power amplifier, an Yb-doped double cladding photonic crystal fiber (DC-200-40-PZ-Yb, NKT Photonics) is pumped with 160 W of radiation from a laser diode yielding 45 W of average output power with sub-200-fs pulses after compression. A pair of transmission gratings (1250 lines/mm) with a total efficiency of 75% is used for compression. A small part of the oscillator output is amplified with an additional fiber amplifier and sent into an $f$-2$f$ interferometer for monitoring the carrier envelope offset frequency ($f_{\mathrm{ceo}}$). The repetition frequency of the oscillator is locked to a rubidium RF standard (FS725, Stanford Research Systems) that is referenced to a GPS receiver by means of a piezoelectric transducer (PZT) actuated mirror installed inside the oscillator cavity. The enhancement cavity is installed in a vacuum chamber and seeded with the output from the power amplifier. One of the highly reflective mirrors in the enhancement cavity is manipulated by a PZT to lock the enhancement cavity onto the laser cavity. To assure long-term operation, a second PZT-actuated mirror in the enhancement cavity compensates for any slow drifts of the cavity length due to thermal effects. When seeding the enhancement cavity with 11 W from the power amplifier, an intracavity power exceeding ∼2 kW is obtained. The lower level of intracavity power compared to our previous report [15] is a result of the bandpass filtering of the oscillator output that is required to force the amplifiers to run at a center wavelength of 1030 nm. The typical pressure inside the generation chamber when operating the Kr gas jet is ∼1 Pa. A Brewster's plate made of single-crystalline MgO with a thickness of 250 $\mu$m is used to couple out the vuv comb from the enhancement cavity. The incident surface of the MgO crystal has a dielectric coating that works as a dichroic mirror with high reflectivity (30% by design) at the 7th harmonic (147 nm) while the loss for the infrared cavity beam is minimized. The outcoupled high harmonic radiation is recollimated by a $CaF_2$ lens and sent into the spectroscopy chamber through a $CaF_2$ window. A dichroic mirror placed after the outcoupler reflects the 7th harmonic radiation, while suppressing the other orders entering the spectroscopy chamber. Inside the spectroscopy chamber, the isotope selected $^{132}$Xe gas is introduced at room temperature from a nozzle with an orifice of 100 $\mu$m with a stagnation pressure of $3 \times 10^{-2}$ bar. Instead of a pulsed gas jet, a continuous xenon beam with a relatively low stagnation pressure was required to suppress the formation of xenon clusters. On the basis of an empirical model [16], we estimate the average cluster size in the xenon gas jet to be much smaller than 2, whereas a pulsed valve with 1 bar of stagnation pressure would result in an average cluster size of 50. The xenon jet is collimated with two molecular skimmers with orifice diameters of 0.2 and 0.4 mm. From the geometry of the skimmers, the full divergence angle of the xenon beam is estimated to be less than 15 mrad. Separated by the skimmers, the three compartments inside the spectroscopy chamber are differentially pumped with four turbo pumps as shown in Fig. 1(b). In the last downstream compartment, the collimated atomic beam interacts with the vuv comb in a perpendicular geometry to suppress Doppler broadening. By guiding an auxiliary He-Ne laser through the two skimmers, the interaction angle is geometrically measured to be $90 \pm 1.5$ deg. The typical background pressure in the interaction region is $\sim 3.5 \times 10^{-6}$ Pa. The fluorescence is photocounted by a vuv-sensitive photomultiplier tube (R1081P, Hamamatsu). In order to extract the weak fluorescence signal from the significantly strong background contribution, due to nonresonant scattering at the vacuum chamber or the entrance window, the photon counting signal is time resolved and the arrival time of the signal is recorded [Fig. 2(a)]. The unwanted background events are expected to be synchronous to the arrival time of the driving laser [region A in Fig. 2(a)]. On the other hand, for excitation with a train of mutually coherent pulses, the fluorescence intensity as a function of time shows both a cw-like component and an exponential decay with a decay time equal to the upper-state lifetime (3.7 ns) that originates from the coherent accumulation of the excited state amplitude [17]. Therefore, the xenon fluorescence can be detected with high

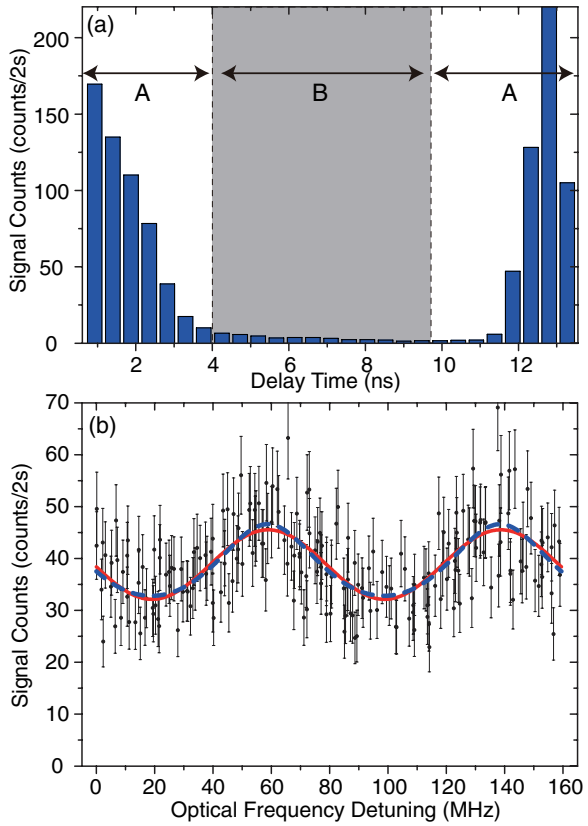


FIG. 2. (Color online) (a) Distribution of the arrival time of the signal. Zero delay is defined to be the arrival time of the excitation pulses. The secondary peak at $f_{\mathrm{rep}}^{-1} \sim 13$ ns corresponds to the counts associated with the next-incoming excitation pulse. The counts inside region B are mainly composed of fluorescence from the xenon atoms, while the peaks in region A contain strong background contributions of unwanted scattering. (b) Typical spectroscopy signal. The measurement was performed with 2 s of integration time for each measurement point. The error bars represent one standard deviation assuming a Poisson distribution of the signal counts. We confirmed that the scattering of the signal obeys a Poisson distribution. See text for the details of solid red and dashed blue curves.

signal to noise ratio by counting the signal inside the time window [4 ns to 10 ns of delay time; region B in Fig. 2(a)], while discarding the background events synchronized to the driving laser [region A in Fig. 2(a)].

To perform comb-resolved spectroscopy, the repetition frequency is scanned, while monitoring the signal counts within in the above-mentioned time window. During the measurement, $f_{\mathrm{ceo}}$ is logged so that the absolute frequency can be determined for each measurement point. The results are shown in Fig. 2(b) as a function of optical frequency detuning. The wavelike modulation of the signal with the period of the repetition frequency reflects the increase (decrease) of the fluorescence when one of the comb modes is on (off) resonance. The dashed blue curve is a fit with a model curve formed by the convolution of a Lorentzian with the comb spectrum. The best fit is obtained when the linewidth of the Lorentzian is set to be 54 MHz, which is 24% larger than the natural linewidth (43 MHz) of the transition [18]. We believe that the broadening is due to residual Doppler width and/or linewidth of vuv comb. Based on the most conservative assumption that the observed broadening is completely determined by the linewidth of our vuv comb, we estimated the comb linewidth to be $\sqrt{54^2 - 43^2} \simeq 31$ MHz assuming the quadratic sum of the linewidths. However, since the residual Doppler width that is expected to be less than 40 MHz for our experimental parameters also contributes to broaden the line, the actual vuv comb linewidth is expected to be smaller than 31 MHz. From the information obtained by a single measurement, the transition frequency can be determined with the uncertainty of the frequency offset given by an integer multiple of the repetition frequency. To determine the absolute frequency, we performed eight measurements with different repetition frequencies ranging from 79.8 MHz to 78.8 MHz. Increasing the range of repetition frequencies would require a complete realignment of the external cavity and would modify the interaction angle between the atomic beam and the comb, which would disrupt the repeatability of the measurements. To determine the absolute frequency and its uncertainty from the obtained data sets, we employed the likelihood method. For the $m$th measurement, the likelihood function $\mathcal{L}_m(\nu_0)$ is defined as

$$\mathcal{L}_m(\nu_0) = \int d\boldsymbol{a} \prod_{n=1}^{N_m} P(f_{\mathrm{model}}(\nu_0, \boldsymbol{a}; \nu_{(m,n)}), y_{(m,n)}).$$

Here, $\mathcal{L}_m(\nu_0)$ stands for the statistical likelihood of obtaining the measured data of the $m$th measurement when the actual transition frequency is assumed to be $\nu_0$. The $m$th measurement contains $N_m$ data points where each optical frequency and the signal counts are given by $\nu_{(m,n)}$ and $y_{(m,n)}$, respectively. The signal counts are assumed to obey a Poisson distribution: $P(\alpha,\beta) = \alpha^{\beta} \mathrm{e}^{-\alpha} (\beta!)^{-1}$. The model curve of the signal counts as a function of the optical frequency $\nu$ is represented by $f_{\mathrm{model}}(\nu_0, \boldsymbol{a}; \nu)$ with $\nu_0$ being the transition frequency and $\boldsymbol{a}$ is a set of other irrelevant parameters of the model curve such as the signal offset. A Lorentzian or Voigt profile convoluted with the comb spectrum should be used as a model curve $f_{\mathrm{model}}(\nu_0, \boldsymbol{a}; \nu)$. However, for the observed modulation depth of the signal, we found that the signal shape is well represented by a pure sinusoidal function as shown by the solid red curve in Fig. 2(b). Therefore, a sine function with a period of the repetition frequency is employed as a model curve for the convenience of the computation. The total likelihood $\mathcal{L}(\nu_0)$ taking into account all eight measurements is defined as $\mathcal{L}(\nu_0) \propto \prod_{m=1}^{8} \mathcal{L}_m(\nu_0)$ and is proportional to the statistical probability of obtaining the measured data sets when the transition frequency is assumed to be $\nu_0$. Note that $\mathcal{L}_m(\nu_0)$ contains $N_m$ measurement points that total likelihood function $\mathcal{L}(\nu_0)$ is composed of $\sum_{m=1}^{8} N_m$ data points.

Figure 3(a) shows the numerical evaluation of $\mathcal{L}(\nu_0)$. This likelihood function has an almost singular peak structure at an optical frequency of 2.04 PHz. Note that the other peaks are at least more than three orders of magnitude smaller in the frequency region from 2.03 to 2.05 PHz. As shown in Fig. 3(b), there are several sharp lines inside the prominent peak structure of the likelihood function with a separation of about the repetition frequency. About six peaks have comparable likelihood, indicating that the comb-mode number is not determined uniquely from the measurement set. However, from the center frequency of the envelope of the

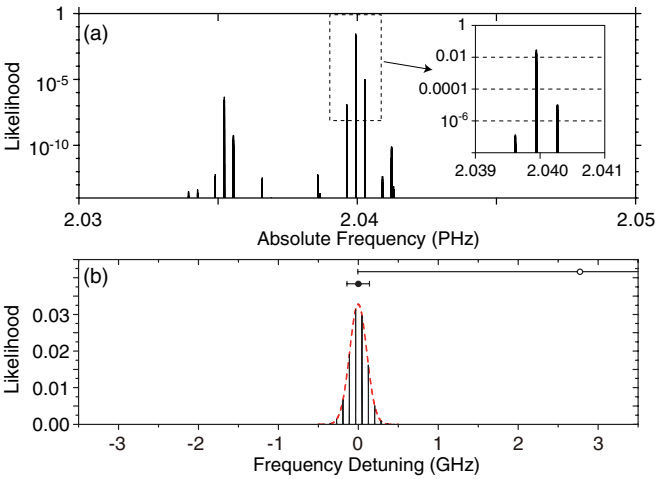


FIG. 3. (Color online) (a) The likelihood for the transition frequency obtained from eight measurements with different repetition frequencies. The inset shows a magnified plot around the highest peak. Note that the plots are in a logarithmic scale and that the highest peak at around 2.04 PHz dominates the likelihood. (b) Magnified plot of likelihood in a linear scale (black). The $x$ axis shows the frequency detuning from 20 39 942.9 GHz. Filled and open dots represent the transition frequency obtained in the current work and in a previous report, respectively [14].

likelihood function [dashed red line in Fig. 3(b)], the absolute transition frequency can be determined. The uncertainty (standard deviation) of the transition frequency is estimated as the 68% confidence interval of the likelihood envelope. After taking into account the uncertainty in the interaction angle measurement between the xenon atomic beam and the vuv comb, the $5p^6$-$5p^5 6s$ transition frequency of $^{132}$Xe is obtained as 20 39 942.91(14) GHz; this is an improvement of more than one order of magnitude in the uncertainty compared with the previous result [14]. Other possible systematic errors (recoil shift, ac Stark effect) are far smaller than our uncertainty.

Instead of the maximum likelihood method as described above, we also performed a conventional data analysis based on the least-squares, Monte Carlo, and linearized error propagation method. The transition frequency and uncertainty agrees with the ones obtained in the maximum likelihood method within ∼10 MHz and ∼15 MHz of difference, respectively, which is an order of magnitude smaller than our measurement uncertainty. Currently, our measurement uncertainty is seriously limited by the ambiguity in the comb mode number determination. Technical improvement in the enhancement cavity setup would allow us to perform measurements with larger detunings of the repetition frequency for a more accurate mode number determination. Based on the previously mentioned conservative estimation of the comb linewidth, we believe that our system has the ability to perform spectroscopy with an accuracy and resolution far better than ∼31 MHz in the vuv region when the comb mode is uniquely identified. With this accuracy, it would be challenging to calibrate the Doppler shift associated with the interaction angle between the xenon beam and the excitation comb.

Our demonstration shows that a relatively simple frequency-comb system referenced and stabilized to a radio frequency standard has sufficient short-term stability to preserve the frequency-comb structure after a highly nonlinear frequency conversion into the vuv via HHG at least up to the 7th order, despite our initial concern that the noise contained in the RF frequency may collapse the coherent comb structure in vuv. As a future prospect, vuv combs can be combined with present spectroscopy techniques such as dual-comb spectroscopy, saturation spectroscopy, and optical lattices, which promise to offer numerous highly interesting applications—for example, vuv optical clocks based on atomic or even nuclear transitions.

This research was supported by the Photon Frontier Network Program of the Ministry of Education, Culture, Sports, Science and Technology, Japan.

[1] C. G. Parthey *et al.*, Phys. Rev. Lett. **107**, 203001 (2011).
[2] S. Blatt *et al.*, Phys. Rev. Lett. **100**, 140801 (2008).
[3] F. Adler *et al.*, Opt. Express **18**, 21861 (2010).
[4] B. Bernhardt *et al.*, Appl. Phys. B **100**, 3 (2010).
[5] N. Leindecker *et al.*, Opt. Express **19**, 6296 (2011).
[6] Ch. Gohle *et al.*, Nature (London) **436**, 234 (2005).
[7] R. J. Jones, K. D. Moll, M. J. Thorpe, and J. Ye, Phys. Rev. Lett. **94**, 193201 (2005).
[8] D. Z. Kandula, Ch. Gohle, T. J. Pinkert, W. Ubachs, and K. S. E. Eikema, Phys. Rev. Lett. **105**, 063001 (2010).
[9] A. K. Mills *et al.*, J. Phys. B **45**, 142001 (2012).
[10] M. Herrmann *et al.*, Phys. Rev. A **79**, 052505 (2009).
[11] D. Kielpinski, Phys. Rev. A **73**, 063407 (2006).
[12] A. Cingöz *et al.*, Nature (London) **482**, 68 (2012).
[13] G. D'Amico, G. Pesce, and A. Sasso, Phys. Rev. A **60**, 4409 (1999).
[14] B. Petersson, Arkiv Fysik **27**, 317 (1964).
[15] A. Ozawa *et al.*, in *Conference on Lasers and Electro-Optics* (Optical Society of America, Washington, DC, 2011), p. CThB4.
[16] J. Wörmer *et al.*, Chem. Phys. Lett. **159**, 321 (1989).
[17] D. Felinto, L. H. Acioli, and S. S. Vianna, Phys. Rev. A **70**, 043403 (2004).
[18] J. Sansonetti *et al.*, *Handbook of Basic Atomic Spectroscopic Data* (National Institute of Standards and Technology, Gaithersburg, MD, 2005).